Hindawi
International Journal of RF and Microwave Computer-Aided Engineering
Volume 2024, Article ID 2028369, 11 pages
https://doi.org/10.1155/2024/2028369

Research Article

Thermal Characteristic Investigation for a Multichip Module Based on APDL

Qian Lin,[1] **Peng-Fei Zhao**,[1] **Rui-lan Yang**,[2] **and Hai-feng Wu**[2]

[1]*School of Physics and Electronic Information Engineering, Qinghai Minzu University, Xining 810007, China*
[2]*Chengdu Ganide Technology, Chengdu 610073, China*

Correspondence should be addressed to Hai-feng Wu; abgott@126.com

Received 26 December 2023; Revised 14 March 2024; Accepted 16 March 2024; Published 17 April 2024

Academic Editor: Paolo Castaldo

Aiming at the failure problems of integrated circuit (IC) caused by higher package density, thinner package, and more heat sources, taking a multichip module (MCM) for receiver front end as an example, the 3-D model is established based on ANSYS Parametric Design Language (APDL). Then, the steady-state thermal analysis is achieved to complete the automatic calculation of thermal characteristic. As a result, the temperature, stress, and deformation are investigated in details, and its temperature distribution, stress distribution, deformation distribution, and reliability variations of this MCM under different powers and temperatures can be obtained. This can provide important theoretical reference for the chip package optimization. Different from other studies which only focus on temperature or stress, it is more comprehensive and systematic for the thermal characteristic analysis of MCM. Meanwhile, this MCM is also representative for wireless communication system. It is of great significance to optimize the layout design and improve the thermal characteristic for IC.

1. Introduction

With the rapid development of mobile communication technology, semiconductor industry has entered the "post-Moore's Law era." The characteristics of high efficiency, high integration, multifunction, and multichannel have become the inevitable trends for chip design [1]. Meanwhile, due to the increase of package chip integration and power density, thermal characteristics of chips are increasingly prominent, which have become one of the important factors affecting the chip reliability.

At present, multichip module (MCM) has been widely utilized for integrated circuit (IC). As the mainstream of multifunction chip, MCM is used to achieve greater wiring density and higher integration [2]. Furthermore, the system characteristic of miniaturization, multifunction, and high performance can be realized by packaging different single-function chips [3]. However, due to the multiple chip packaging, the number of heat sources and power density in MCM is increasing. The accumulation of heat and changes in internal temperature are caused by more dissipated power. As a result, chip performance will be reduced [4]. In addition, because it contains different materials and thermal properties, thermal stress and thermal deformation can be produced by temperature mutation. Ultimately, the lifetime is reduced, and the structure is destroyed of the MCM by stress and deformation [5, 6]. Therefore, it is necessary and urgent to investigate the thermal characteristics of MCM.

As the main factor for IC reliability, thermal characteristics have received extensive attentions in recent decades. In 2004, Wilkerson et al. proposed the temperature analysis for radio frequency (RF) circuits based on the finite element analysis (FEA). It converts the circuit interconnect into heat conduction block to improve calculation speed and accuracy [7]. In 2004, Wang and Zhou implemented the static thermal-electric coupling simulation by using the decoupling iteration method. The steady-state operating temperature and characteristics of the circuit were solved [8]. In 2010, the finite element modeling and simulation of electromigration (EM) failure for a COMS inverter were completed by He and Tan [9]. In 2017, Lin et al. completed

interconnect reliability analysis for the GaAs monolithic microwave integrated circuit (MMIC) power amplifier (PA) with different currents and gate widths [10]. In 2019, Wei et al. conducted fluid-structure analysis by coupling finite element model (FEM) for MCM [11]. Meanwhile, Yang and Pan studied the influence of the power distribution of two-layer chips and the number of chips on the temperature field on the PCB board [12]. In 2020, Gong et al. established a three-dimensional model combining multichip components and ball gate array and analyzed the thermal and fluid flow properties considering microchannel heat sink and heat source [13]. In 2021, the EM failure of a stacked distributed PA was analyzed with different conditions [14]. Then, the interconnect reliability investigation was achieved for a high-power GaN MMIC PA [15].

Now, most studies of thermal characteristics only focus on temperature distribution without comprehensive analysis. However, the thermal characteristics of the chip include temperature, thermal stress, and the thermal deformation, which are of great significance to the layout and reliability design of integrated circuits (ICs). In addition, with the universality and severity of thermal reliability, the perfect and efficient MCM thermal characteristic analysis method is urgently needed. Therefore, automatic modeling and analysis are used to achieve the comprehensive thermal reliability study for a highly integrated dual-channel MCM in this paper. This is the continuation and further exploration for IC reliability.

In this paper, based on FEA and ANSYS Parametric Design Language (APDL), 3-D automatic modeling of MCM consisting of two Si switch chips and two GaAs low noise amplifiers is achieved. The automatic calculation of thermal characteristics can be achieved with FEA. The detailed thermal analysis process is presented here. Considering the heat generation rate, heat dissipation, and heat radiation of the MCM, the distribution and tendency of temperature, thermal stress, and thermal deformation under different temperatures and powers can be analyzed. Ultimately, the factors affecting thermal characteristics of MCM are determined, which can provide a theoretical basis for the package optimization and reliability design for IC.

2. Thermal Analysis Theory

Thermal characteristics are considered to be the main factors for the package reliability. It includes temperature, stress, and deformation. Firstly, due to the existence of temperature gradient and different thermal expansion coefficient, the stress and deformation can be generated. Stress concentration can cause the destroy of MCM structure, and deformation can bring the layered image between the package layers [16]. Finally, this can cause the deformation and failure of device. In addition, the temperature impact for IC reliability cannot be ignored. The higher the temperature, the smaller the reliability and lifetime of chip [17]. Therefore, it is necessary to focus on the thermal characteristics of MCM. If the influence of thermal characteristics can be fully considered in chip design, the necessary measures should be taken. It can ensure the reliability of MCM within all the working conditions.

Temperature is related to a variety of physical factors. In order to better simulate the internal and external environment of the MCM, it is necessary to define multiple physical parameters to achieve load application, such as operating temperature, heat production, and other parameters. The dissipated power (Q) of chip can be given by equation (1) in [14].

$$Q = P_{\mathrm{DC}} \times (1 - \eta) = I_{\mathrm{DC}} \times V_{\mathrm{DC}} \times (1 - \eta), \tag{1}$$

where P_{DC} is DC power, η is power added efficiency, I_{DC} is DC current, and V_{DC} is DC voltage. If the internal chips of MCM are regarded as the heat source, the unit heat generation rate can be given by (2) in [14].

$$H = \frac{Q}{V}, \tag{2}$$

where H is the heat generation rate and V is the chip volume.

In addition, the change of temperature can cause thermal stress and thermal deformation. From the perspective of thermal characteristics, it is mainly related to temperature distribution and thermal expansion coefficient and its structure. As long as the mechanical response of the object does not affect the thermal performance and boundary conditions, thermal analysis can be decomposed into temperature analysis and structural static analysis [17]. As a result, the heat transfer equation in the steady-state system can be expressed as

$$\frac{\partial}{\partial x}\left(k_x \frac{\partial T}{\partial y}\right) + \frac{\partial}{\partial y}\left(k_y \frac{\partial T}{\partial y}\right) + \frac{\partial}{\partial z}\left(k_z \frac{\partial T}{\partial z}\right) + \rho H = 0, \tag{3}$$

where T is temperature, H is heat generation rate, ρ is density, and k_x, k_y, and k_z are the thermal conductivity in the x, y, and z directions, respectively. Simplify equation (1) as follows:

$$KM = B, \tag{4}$$

where M is the conduction matrix, including thermal conductivity and convection coefficient, K is the node temperature vector, and B is the node heat flow rate vector. As a result, the relationship between the thermal deformation and thermal stress can be described by the following formula [7, 18]:

$$\sigma = D\varepsilon, \tag{5}$$

$$\varepsilon = \alpha(T - T_{\mathrm{ref}})[111000]^T, \tag{6}$$

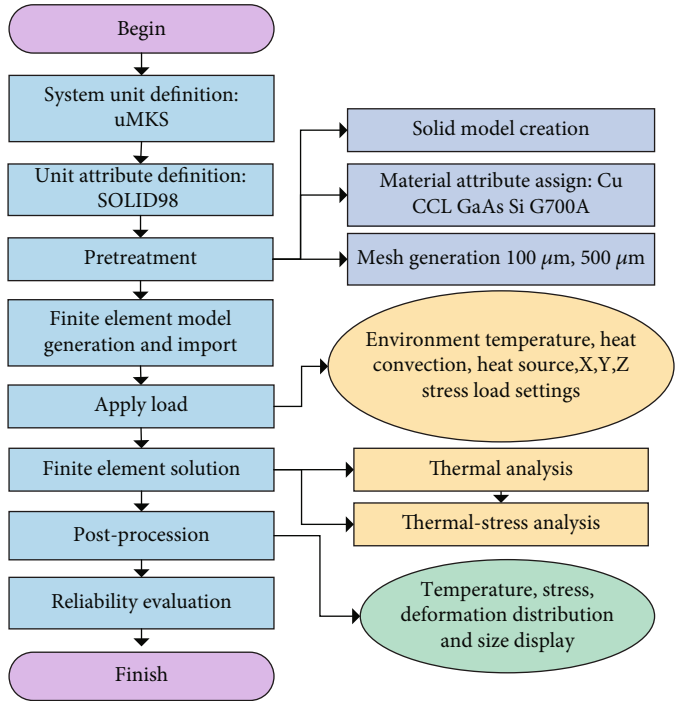

Figure 1: Flowchart of MCM thermal analysis.

$$D = \frac{E}{(1+\nu)(1-2\nu)} \begin{bmatrix} 1-\nu & \nu & \nu & 0 & 0 & 0 \\ \nu & 1-\nu & \nu & 0 & 0 & 0 \\ \nu & \nu & 1-\nu & 0 & 0 & 0 \\ 0 & 0 & 0 & 1-\nu & 0 & 0 \\ 0 & 0 & 0 & 0 & 1-\nu & 0 \\ 0 & 0 & 0 & 0 & 0 & 1-\nu \end{bmatrix}, \quad (7)$$

where σ is the stress, ε is the deformation, D is the elastic matrix, α is the thermal expansion coefficient, T_{ref} is the deformation reference temperature, E is the elastic modulus of the material, and ν is the Poisson ratio.

Based on the formulas above, the calculation for MCM thermal characteristics can be accomplished. Furthermore, APDL is used to complete the thermal stress analysis. Then, the temperature, stress, and thermal deformation distribution of MCM can be obtained. APDL is an interpreted language similar to FORTRAN [19], which can achieve the functions such as parametric 3-D modeling, load apply, and solution. The automatic construction and coupling analysis of temperature, thermal stress, thermal conductivity coefficient, thermal expansion coefficient, Young's modulus, Poisson's ratio, and other parameters can be realized by APDL.

The flowchart of thermal analysis for MCM is shown in Figure 1. It can be divided into three parts: pretreatment, solution, and general postprocession. Pretreatment is mainly for 3-D modeling and meshing. It includes the definitions of system units, properties, and materials. The solution mainly includes applying boundary and constraint conditions, thermal analysis, thermal deformation analysis, and calculation. Finally, the postprocession is used to display for solution results and reliability evaluation.

3. 3-D Modeling of MCM

An RF MCM for a time division duplex base station is taken as an example to construct the 3-D model. Figure 2 is the architecture diagram of this MCM chip, which mainly integrates two low noise amplifiers (LNAs) with 0.25 μm GaAs pHEMT and two high-power switching chips with 0.18 μm SOI. It covers the bands below 6 GHz with a noise factor of 1.4 dB in receive mode. The maximum input power can reach to 39 dBm with the package size of 6 mm × 6 mm. Moreover, the MCM has two channels, such as RF-IN-A and RXOUT-A and RF-IN-B and RXOUT-B.

The physical photo of MCM with the mixed-class package is shown in Figure 3. It adopts LGA substrate with 40-pin and is powered by positive voltage and single power. Inside the MCM, it is connected with four layers of interconnect substrate which plays the role of current conduction and support. The insulating material of the substrate is epoxy resin compound, and its conductor material is copper. Meanwhile, the copper surface is plated with nickel palladium gold. The outer package is the plastic encapsulation material of G700A including epoxy resin, curing agent, and spherical silica filler. Figure 3 is the MCM physical photo containing the PCB.

Due to the complex structure of MCM, some simplifications are carried out without affecting the analysis results. Therefore, the dense interconnect is transformed into equivalent heat conduction block based on power consumption. In addition, the structure and material with the greatest influence factors are extracted according to the MCM layout.

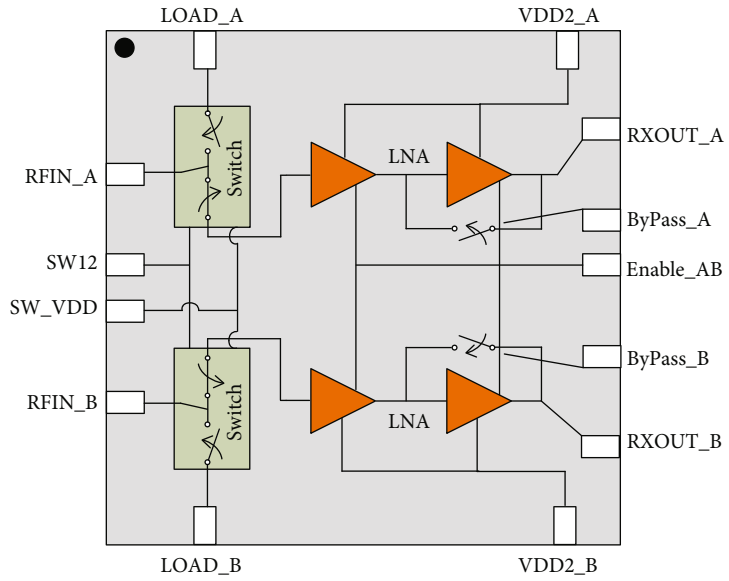

Figure 2: Architecture diagram of the MCM.

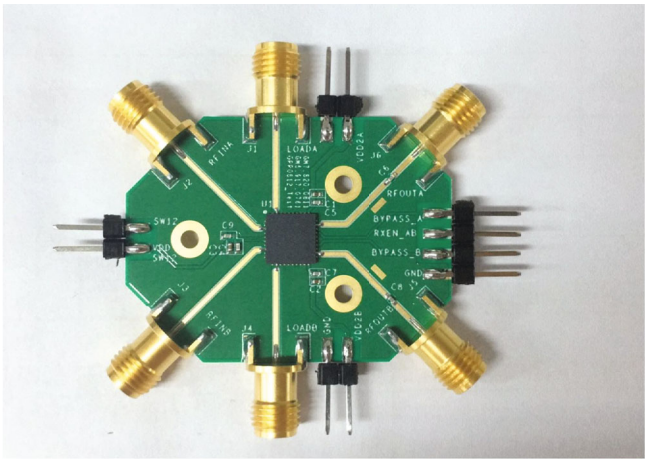

Figure 3: Physical photo of MCM.

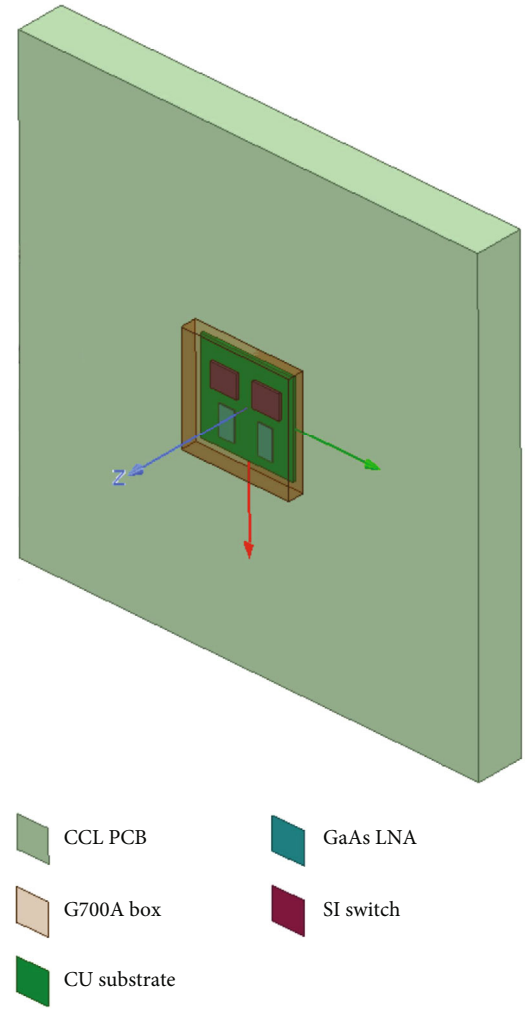

Figure 4: 3-D model of the whole MCM.

The simplified MCM model including the PCB, the overall sealing box, the substrate, two switch, and two LNA chips is shown in Figure 4. Meanwhile, the corresponding material properties are added to each module to ensure the accuracy of the analysis. Thus, the cost of analysis can be reduced, and the efficiency was improved by simplifying the model. In addition, the geometric size of the PCB is $40 \times 40 \times 3$ mm, the box size is $6 \times 6 \times 0.55$ mm, the substrate size is $5.9 \times 5.9 \times 0.2$ mm, the LNA size is $1.9 \times 1 \times 0.075$ mm, and the switch chip size is $1.5 \times 1.7 \times 0.15$ mm.

Based on the MCM structure mentioned above, FEA pretreatment is achieved here. Furthermore, SOLID98 is used as the cell, which is a three-dimensional tetrahedral entity unit. Each tetrahedral unit contains 10 nodes, including four corner nodes and six edge nodes. It also contains six degrees of freedom such as temperature, stress, and deformation, which can meet the calculation of thermal characteristic analysis. The system unit is defined as umks metric

Table 1: Material attributes for MCM model.

Material	Density (g/cm^3)	Thermal expansivity (1/°C)	Specific heat (J/kg°C)	Coefficient of heat conduction (W/m°C)	Young's modulus (MPa)
Cu	8.92	1.65×10^{-5}	385	401	1.29×10^5
CCL	1.93	1.8×10^{-5}	1280	1.2	1.1×10^4
GaAs	5.31	3.1×10^{-6}	360	130	3.9×10^5
Si	2.33	2.6×10^{-6}	700	149	1.3×10^5
G700A	1.99	1×10^{-5}	1064	0.96	5400

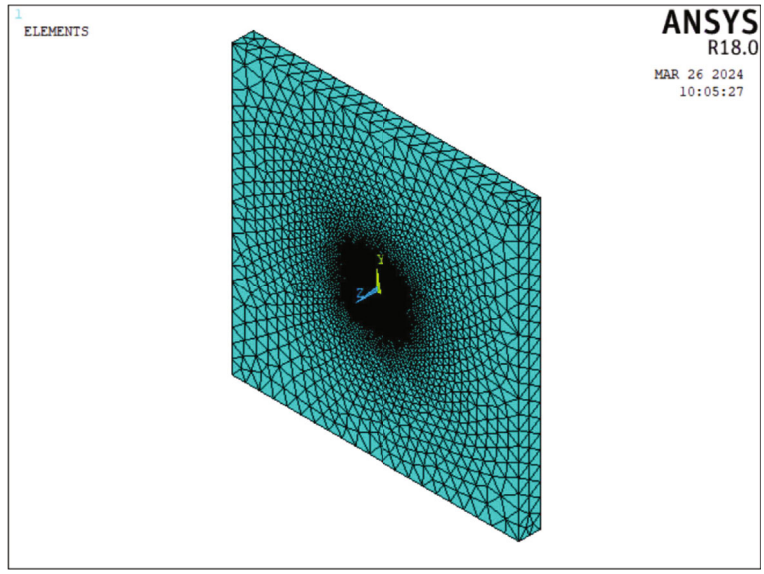

Figure 5: Meshing result of MCM 3-D model.

(kg, μm, s, °C, mA, μN, and V). It is worth noting that the material properties of the model are shown in Table 1, including copper, GaAs, silicon, plastic sealing materials G700A, and plate CCL.

After the 3-D modeling is constructed, its material properties need to be defined for the different solid models. Here, the corresponding material properties are added to each part of the model according to its process as shown in Table 1. Meanwhile, the free grid division method is adopted here; it can automatically generate tetrahedral mesh on the volume. The size and density distribution of the mesh can be controlled manually. This meshing method is easy to set up and highly automated. Therefore, the model is divided into submodel and overall model. The submodel is refined, and the overall model is coarse. The mesh size of the submodel is 100 μm, and the mesh size of the overall model is 500 μm. This can ensure the efficiency and accuracy for FEA. The result of grid division is shown in Figure 5. The number of cell nodes is 490126, and the grid division is good. Finally, its FEM is generated for the next thermal analysis.

It is worth noting that the APDL is used to construct the model based on a total of 189 APDL statements within only 20 seconds. The time of 3-D modeling and resource can be dramatically reduced. As a result, the subsequent circuit reliability analysis can be guaranteed.

4. Results and Discussions

When analyzing the thermal characteristics of MCM, heat source and temperature are the primary factors. Therefore, temperature, stress, and deformation of MCM under different powers and temperatures are analyzed here. In details, the thermal characteristic analysis for MCM is divided into two parts: thermal analysis and thermal stress analysis [17]. Meanwhile, the automatic finite element solution can be achieved by APDL command flow.

According to formulas (1)–(7), the results of temperature, stress, and deformation are jointly caused by thermal conductivity, thermal expansion coefficient, elastic modulus, Poisson's ratio, and thermal convection coefficient. Therefore, in order to calculate the thermal characteristics, the material properties, initial conditions, and constraints must be determined. For a receiver front-end MCM chip, the ambient temperature in the base station is usually set at -5 to 45°C. However, in some cases, due to the heat dissipation of the surrounding devices, the ambient temperature of the MCM may be increased. Therefore, the thermal

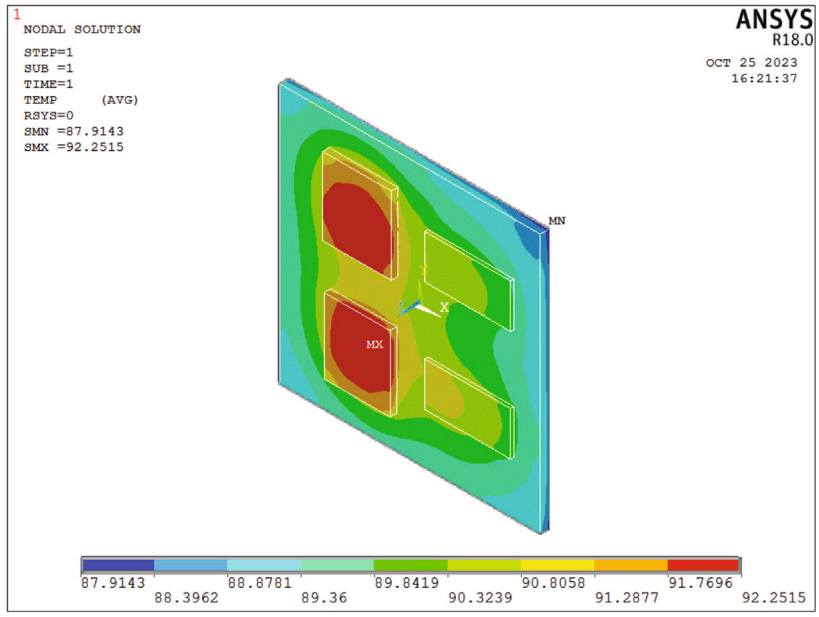

Figure 6: Temperature distribution of internal chip when T = 70°C and PWR = 6 W.

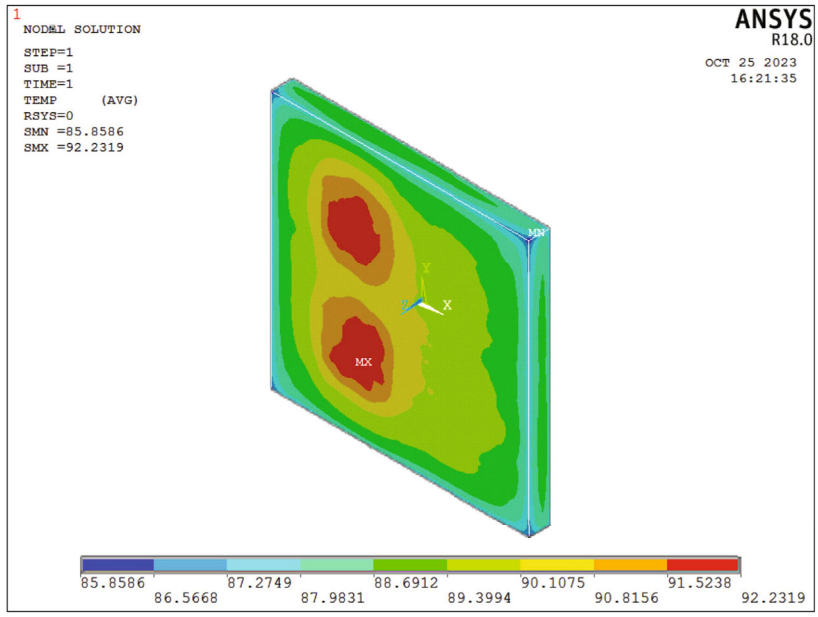

Figure 7: Temperature distribution of the whole chip when T = 70°C and PWR = 6 W.

characteristics of MCM at ambient temperatures ranging from -10 to 70°C are studied here.

Taking the ambient temperature of 25°C and the power of 6 W as an example, the initial temperature load of all nodes is set to 25°C, respectively, and the air temperature is constant to 25°C. Secondly, the heat convection and heat radiation with the convection coefficient h of 20 W/(m^2·°C) are also set on the outer surface for the model. Finally, the unit heat production of the internal chip is calculated by formulas (1) and (2), and the unit heat generation rate is about 0.4 W/mm^3. Ultimately, the temperature distribution of MCM can be calculated based on the full constraint conditions for the bottom and around the MCM plate.

For the thermal stress analysis, it is also necessary to set the initial temperature and air temperature. Secondly, the reference temperature and the displacement constraint conditions should be set at the bottom and around the MCM plate for the thermal stress calculation. Meanwhile, the initial stress deformation of all nodes in the X, Y, and Z directions is set to 0. Finally, the temperature result is introduced into the thermal stress analysis to calculate the stress deformation.

The power (PWR) range of MCM is about 1 W~10 W, and 6 W is selected as the load here. The temperature distribution with T of 70°C and PWR of 6 W is shown in Figure 6. It can be seen that the isotherm line decreases in a circular direction from the heat source as the center. The highest

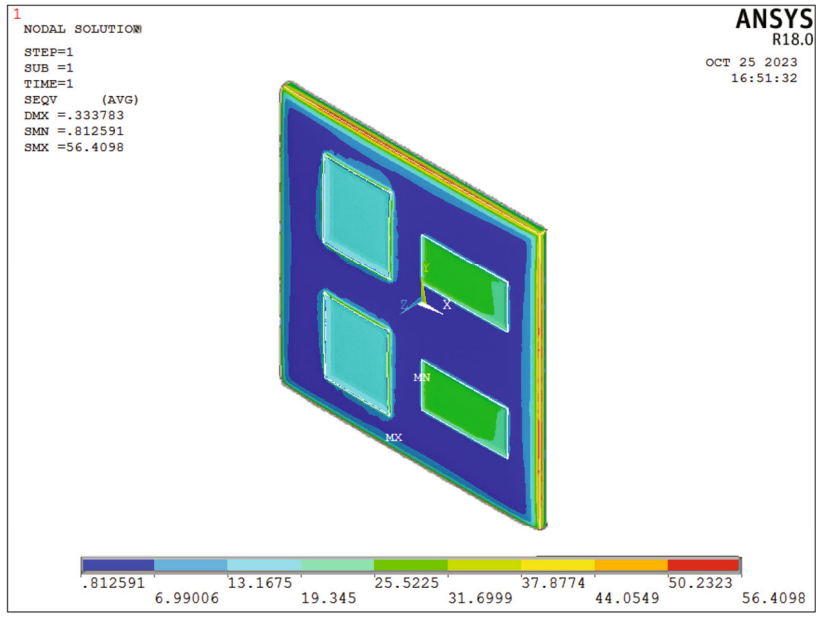

Figure 8: Stress distribution of internal chip when $T = 70^{\circ}C$ and PWR = 6 W.

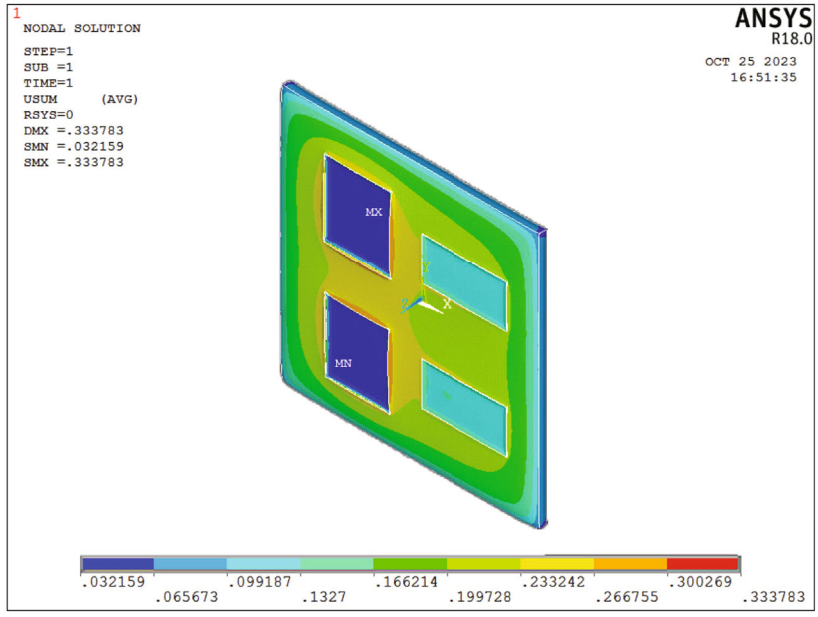

Figure 9: Thermal deformation distribution of internal chip when $T = 70^{\circ}C$ and PWR = 6 W.

temperature at the heat source of the chip is 92.25°C, while the lowest temperature around the MCM substrate is 87.9°C. That is to say, the temperature difference is about 5°C for the whole chip.

Figure 7 shows the temperature distribution of the whole chip with T of 70°C and PWR of 6 W. It can be seen that the highest temperature is about 92.23°C and the lowest temperature is about 85.8°C. The high temperature of the plastic sealing material is mainly concentrated in the middle of the shell part close to the chip. This is due to the poor thermal conductivity of the plastic sealing material, which is not conducive to the heat generated by the chip to be distributed outward. Ultimately, the temperature of plastic sealing material close to the chip is too high.

Based on the established 3-D model, the aforementioned temperature load is applied to the 3-D model as the volume load. The stress distribution diagram of internal chip with T of 70°C and PWR of 6 W is shown in Figure 8. It can be seen that the stress variation is significantly at the edge and corner of the whole chip. The maximum occurs at the joint around the substrate and the plastic sealing material. This is because the substrate and the plastic sealing material have

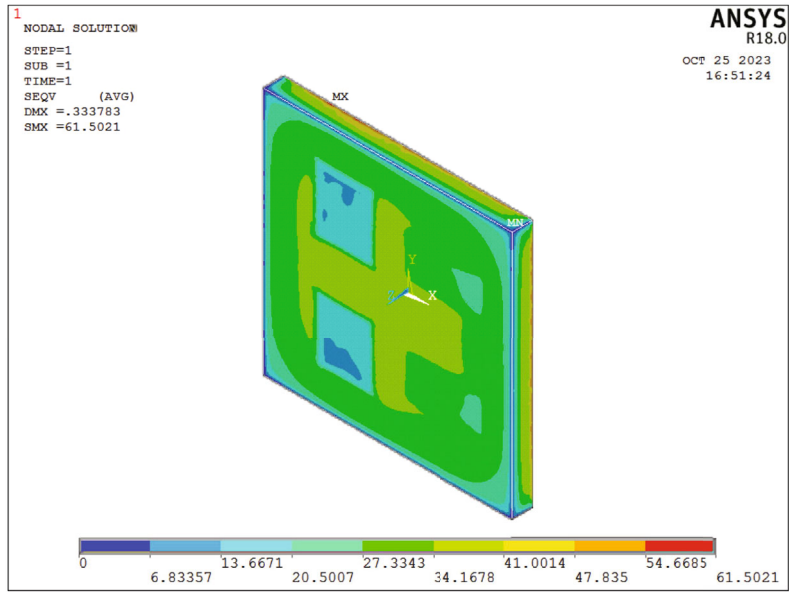

FIGURE 10: Stress distribution of the whole chip when $T = 70^{\circ}C$ and PWR = 6 W.

different thermal expansion coefficient, heat conduction, and other material properties, resulting in uneven temperature distribution and different size deformation. Meanwhile, it can be seen that the thermal gradient between the substrate and the plastic sealing material is large. It ultimately causes the stress distribution to be concentrated in its contact position.

Figure 9 shows thermal deformation distribution of internal chip with T of 70°C and PWR of 6 W. It can be seen that the highest deformation of the MCM is about 0.334 μm and the lowest deformation is about 0.032 μm. The center of the entire size has an upward trend. The overall displacement is large in the middle and small in the periphery. It changes layer by layer from inside to outside. The maximum deformation position is concentrated on the upper surface of the substrate and the contact position between the inner chip and substrate. This is related to the thermal characteristics of the material. In detail, due to the different thermal expansion coefficients of the material and the temperature difference, the deformation of the contact is larger. Therefore, better materials can be used to improve the performance and reliability of chip.

The stress distribution of the whole MCM with T of 70°C and PWR of 6 W is shown in Figure 10. It can be seen that the highest stress of the MCM is about 61.5 MPa and the lowest stress is about 85.8 MPa. The stress changes significantly at the bottom edge of the plastic sealing material, and the stress is relatively concentrated. This is because the deformation is constrained at the position where the plastic sealing material meets the plate. Due to the different properties of the materials, the temperature distribution is uneven and the size deformation is different. Ultimately, the stress distribution is concentrated at the bottom of the plastic sealing material.

When analyzing the influence of power on the thermal characteristics, only the dissipated power is changed while keeping other solution settings. The power variation range of 1 W to 10 W is selected here. Figure 11 shows the curves of maximum thermal stress and thermal deformation with different powers. It can be seen that when the power increases from 1 W to 10 W, the thermal stress rises about 90 MPa and the thermal deformation increases by about 5.1×10^{-4} mm. With the increasing of power, MCM thermal stress and thermal deformation change greatly. Therefore, it is necessary to reduce the dissipated power as much as possible to ensure higher output efficiency.

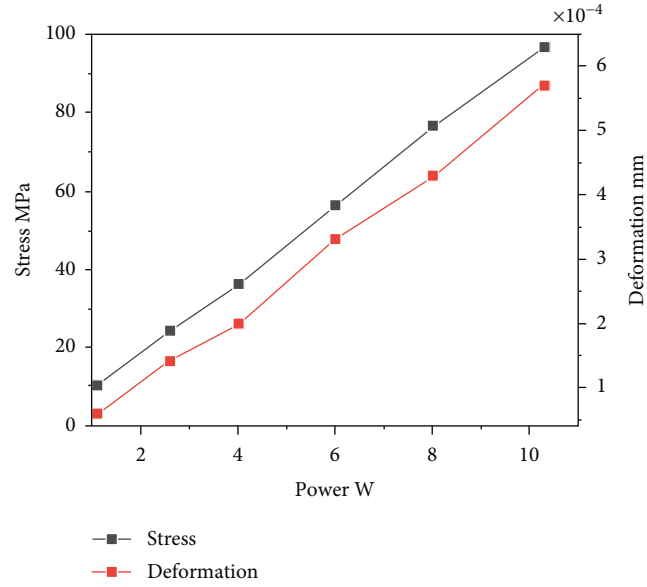

FIGURE 11: Curves of maximum thermal stress and thermal deformation with different powers when $T = 70^{\circ}C$.

Figure 12 shows the curves of maximum temperature and temperature difference with different powers. It can be seen that when the power increases from 1 W to 10 W, the

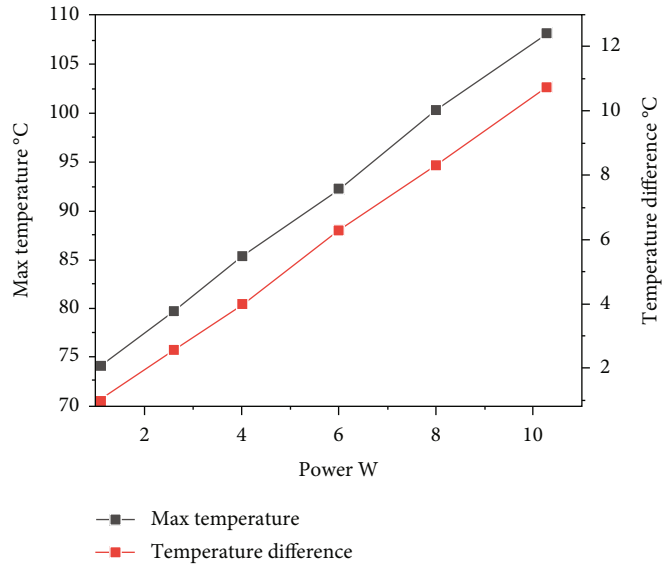

Figure 12: Curves of maximum temperature and temperature difference with different powers when $T = 70^{\circ}C$.

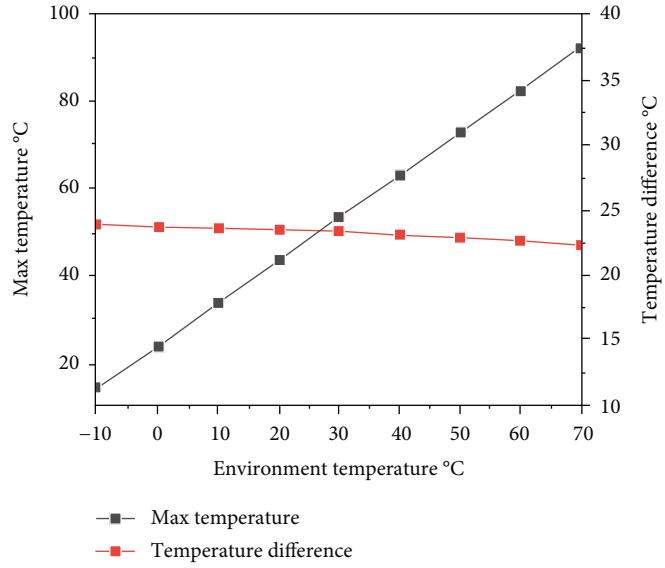

Figure 13: Curves of maximum temperature and temperature difference with different temperatures when PWR = 6 W.

maximum temperature and temperature difference increase linearly. The maximum temperature rises by nearly 35°C, and the difference between the maximum temperature and the initial temperature is 40°C.

When analyzing the influence of different temperatures on the thermal characteristics, only the temperature is changed while keeping other parameters constant. Moreover, the temperature is selected from -10°C to 70°C. The curves of maximum thermal stress and thermal deformation difference, maximum temperature, and temperature difference when PWR is 6 W are shown in Figures 13 and 14, respectively. It can be seen from Figure 13 that the maximum temperature of MCM has an increase linear relationship with temperature. The maximum temperature difference on the MCM panel is basically unchanged.

Meanwhile, it can be seen from Figure 14 that the difference of thermal stress and thermal deformation does not change significantly with the increase of ambient temperature. This is because the factors that affect the final difference of stress and deformation are the difference between the maximum temperature and the initial temperature and the heat distribution. The factor causing the temperature difference is the change in power, and it can be seen from Figure 13 that the initial temperature has little influence on the temperature difference. Therefore, the stress and deformation difference also changes little with the initial temperature.

According to the above results, the maximum temperature, thermal stress, and thermal deformation increase obviously with the increasing power. The maximum temperature increases linearly with the increasing temperature. The

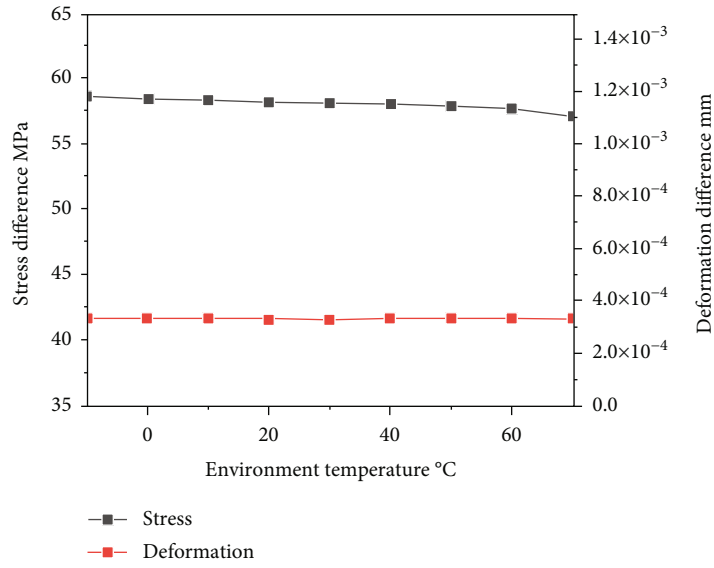

Figure 14: Curves of maximum thermal stress difference and thermal deformation difference with temperatures when PWR = 6 W.

changes of thermal stress and thermal deformation difference of MCM are negligible with the temperature range of -10°C to 70°C. Comparing the results of three groups, it can be found that the change of thermal stress and thermal deformation mainly depends on the temperature gradient of MCM. With the increase of temperature gradient, its thermal stress and thermal deformation increase correspondingly.

Meanwhile, the experiment results show that combing the APDL program and cyclic command flow to complete the FEA of thermal characteristics is more efficient and time-saving. Compared to the cumbersome WORKBENCH analysis, a lot of duplication work can be reduced. Moreover, the file size of APDL is generally only a few tens of kB and its data volume is much lower than that of WORKBENCH. In addition, since the type of the APDL file is the txt, it is possible to run and transfer the file in different operating systems and different software versions.

5. Conclusions

Based on the FEA and APDL, the thermal characteristics of MCM with different powers and temperatures are analyzed automatically. A detailed thermal characteristic analysis is presented for a MCM chip. The temperature, thermal stress, and thermal deformation of MCM can be quantified. It can be seen that the stress changes obviously at the edge and corner of the chip. The maximum appears at the connection between the substrate and the plastic sealing material. Moreover, the temperature is decreasing from center to the edge. The deformation has the maximum at the connection between the switch chip and substrate. It can be concluded that the influence of power on thermal stress and thermal deformation is greater than that of temperature. Therefore, the layout design needs to be optimized appropriately, such as increasing the angle or changing the shape of the device. Meanwhile, it is wise to increase the distance between multiple chips and reduce the thickness of the plastic sealing material. Moreover, the heating device should be placed near the airflow channel as much as possible. In sum, this can provide valuable theoretical guidance for package optimization and reliability design of IC.

Data Availability

The data used to support the findings of this study are included within the article.

Conflicts of Interest

The authors declare that they have no conflicts of interest.

Acknowledgments

The authors gratefully acknowledge financial support by the National Natural Science Foundation (62161046) and the West Light Youth Talent Program of the Chinese Academy of Sciences (1_14).

References

[1] R. R. Schaller, "Moore's law: past, present and future," *IEEE Spectrum*, vol. 34, no. 6, pp. 52–59, 1997.

[2] Y. Y. Wang and Y. Cheng, "Research on 3D-MCM practical technology based on MCM-C process," *Microelectronics*, vol. 44, no. 6, pp. 818-819, 2014.

[3] Q. Lin, L. Jia, H. Wu, and X. Wang, "Investigation on temperature behavior for a GaAs E-pHEMT MMIC LNA," *Micromachines*, vol. 13, no. 7, p. 1121, 2022.

[4] B. Ding, Z. H. Zhang, L. Gong, C. Y. Zhu, and M. H. Xu, "Coupling management optimization of temperature and thermal stress inside 3D-IC with multi-cores and various power density," *International Communications in Heat and Mass Transfer*, vol. 120, article 105021, 2021.

[5] A. Darwish, A. J. Bayba, and H. A. Hung, "Channel temperature analysis of GaN HEMTs with nonlinear thermal

conductivity," *IEEE Transactions on Electron Devices*, vol. 62, no. 3, pp. 840–846, 2015.

[6] P. Shi and Y. N. Chen, "Research on semi-analytical thermal analysis of multi-layer cylindrical electronic module," *Acta Electronica Sinica*, vol. 29, no. 8, pp. 1121-1122, 2001.

[7] P. Wilkerson, A. Raman, and M. Turowski, "Fast, automated thermal simulation of three-dimensional integrated circuits," in *The Ninth Intersociety Conference on Thermal and Thermomechanical Phenomena In Electronic Systems (IEEE Cat. No.04CH37543)*, pp. 706–713, Las Vegas, NV, USA, June 2004.

[8] N. L. Wang and R. D. Zhou, "Electromigration reliability diagnosis and clock integrity analysis based on electrothermal simulation," *Journal of Tsinghua University*, vol. 31, no. 7, pp. 984–987, 2004.

[9] F. He and C. M. Tan, "Electromigration reliability of interconnections in RF low noise amplifier circuit," *Microelectronics Reliability*, vol. 52, no. 2, pp. 446–454, 2012.

[10] Q. Lin, H. Wu, S. J. Chen, G. Jia, W. Jiang, and C. Chen, "Study of complete interconnect reliability for a GaAs MMIC power amplifier," *International Journal of Electronics*, vol. 105, no. 5, pp. 794–805, 2018.

[11] H. Wei, C. Huang, and L. Ying, "Analysis of thermal stress and strain in BGA solder joint based on microchannel ceramic substrate," *IEEE Transactions on Components, Packaging and Manufacturing Technology*, vol. 9, no. 5, pp. 895–904, 2019.

[12] Z. Q. Yang and Z. L. Pan, "Optimization of 3D stacking chip thermal layout based on genetic particle swarm algorithm," *Electronic Process Technology*, vol. 40, no. 5, pp. 249–252, 2019.

[13] L. Gong, Y. P. Xu, B. Ding, Z. H. Zhang, and Z. Q. Huang, "Thermal management and structural parameters optimization of MCM-BGA 3D package model," *International Journal of Thermal Sciences*, vol. 147, no. 10, article 106120, 2020.

[14] Q. Lin, H. F. Wu, L. Zhu, X. M. Zhang, and L. S. Liu, "Design and electromigration study for a stacked distributed power amplifier," *Journal of Circuits, Systems and Computers*, vol. 30, no. 7, article 2150116, 2021.

[15] Q. Lin, P. F. Zhao, H. F. Wu, and S. W. Chen, "Interconnect reliability investigation for a high power GaN MMIC PA based on APDL," *International Journal of RF and Microwave Computer-Aided Engineering*, vol. 32, no. 12, Article ID e23552, 2022.

[16] G. Deng, Z. Li, N. Yan, Y. Zhang, and J. Qiu, "Failure mechanism of interfacial thermal stress of MCM," in *2014 10th International Conference on Reliability, Maintainability and Safety (ICRMS)*, pp. 257–262, Guangzhou, China, August 2014.

[17] S. Zhou and J. Wang, "An experimental investigation of the degradation of CMOS low-noise amplifier specifications at different temperatures," *Micromachines*, vol. 13, no. 8, p. 1268, 2022.

[18] G. Nan, Z. H. Xie, X. N. Guan, Z. Q. Lu, and Y. L. Ge, "Constructal optimization for the layout of multi-chip module based on thermal-flow-stress coupling calculations," *Semiconductor Optoelectronics*, vol. 42, no. 5, pp. 678–685, 2021.

[19] E. Madenci and I. Guven, *The Finite Element Method and Applications in Engineering Using ANSYS®*, Springer, 2015.